Diffusivity of rocks: Gas diffusion measurements and correlation to porosity and pore size distribution

Sheng Peng,[1] Qinhong Hu,[1] and Shoichiro Hamamoto[2]

Received 27 June 2011; revised 28 December 2011; accepted 5 January 2012; published 9 February 2012.

[1] Diffusivity was measured for 12 rock and construction material samples using a diffusion chamber method with oxygen as the tracer gas. Several steps were implemented to minimize leakage between the sample and the core holder, and rigorous tests were performed to evaluate and correct the overall leakage of the diffusion apparatus. This method was proven capable of rapidly measuring the diffusion coefficient for consolidated samples having dimensionless diffusivity values greater than 4.7×10^{-4} in a relative short duration (hours to 1 day). Gas diffusion measurements were also conducted for 11 repacked sediments and sands. Our results are consistent with literature data from liquid tracer through-diffusion methods; the diffusivity versus porosity relationship for our data can be described by Archie's law. The m value in Archie's law was found to be correlated to pore size: the finer the pore size is, the larger the m value is. A linear regression equation can describe the change of m with ln d_{50} (the volumetric mean pore diameter) for most rocks with $d_{50} < 1.3$ μm, while the outliers can be correlated to narrower pore size distribution.

Citation: Peng, S., Q. Hu, and S. Hamamoto (2012), Diffusivity of rocks: Gas diffusion measurements and correlation to porosity and pore size distribution, *Water Resour. Res.*, *48*, W02507, doi:10.1029/2011WR011098.

1. Introduction

[2] Diffusion in rock, of either gas or liquid phase, could be the rate-limiting or dominant process in many scenarios, such as geologic disposal of radioactive waste [*Gillham et al.*, 1984], contaminant remediation [e.g., *Becker and Shapiro*, 2000], CO_2 geological sequestration [*Hatiboglu and Babadagli*, 2010], and oil and gas recovery [*Cui et al.*, 2004, 2009]. Diffusion of hazardous gas or liquid chemicals in construction materials has also become a concern for public health and security [*Nestle et al.*, 2001a, 2001b; *Conca et al.*, 2004]. Therefore, knowledge of diffusion processes and rates in rock is important to a better understanding of these problems.

[3] Diffusivity has been measured using either gas phase or liquid phase tracer methods. The Wicke-Kallenbach cell and Graham's diffusion cell are commonly used for gas diffusion characterization of chemical engineering materials [*Hou et al.*, 1999; *Mouchot and Zoulatian*, 2002; *Zhang et al.*, 2004; *Schlünder et al.*, 2006; *Salejova et al.*, 2011]. However, measurements with these cells require strictly isobaric conditions in cell compartments. *Soukup et al.* [2008] indicated that even a small pressure difference (7–9 Pa) can lead to a significant diffusion flux deviation for samples with pores larger than 7 μm. This can be problematic for geological porous media having pores larger than 7 μm, while it is challenging to achieve a strict isobaric condition.

[4] Diffusivities for a limited number of rock samples, using the liquid tracer method, have been reported [e.g., *Boving and Grathwohl*, 2001; *Polak et al.*, 2002]. However, the experimental duration is long because of the slow diffusion rate of a liquid tracer; even for porous limestone and sandstone samples, the diffusion experiment lasted from 7 days to over 46 days [*Boving and Grathwohl*, 2001]. The NMR (nuclear magnetic resonance) technique has been used to determine gas transport parameters including permeability, diffusion coefficient, and tortuosity with xenon gas [*Mair et al.*, 2001; *Wang et al.*, 2004, 2005; *Newling*, 2008]. A weakness of this technique is that it is not applicable to samples with heavy paramagnetic impurities or other properties that produce high background magnetic gradients [*Wang et al.*, 2005]. In addition, the general lack of readily available access to the NMR facilities limits its application.

[5] On the other hand, gas diffusivity measurements in unconsolidated media with variable saturations, using a diffusion chamber method, are well established in soil science [*Rolston and Moldrup*, 2002]. The approach has been utilized in studies of soil samples representing a wide range of soil types because of its simplicity and accuracy of measurement [e.g., *Shimamura*, 1992; *Freijer*, 1994; *Moldrup et al.*, 2007; *Hamamoto et al.*, 2010, 2011; *Kristensen et al.*, 2010]. Both repacked and undisturbed samples for sandy soil, loamy-clayey soil, volcanic ash soils under different water saturations [*Hamamoto et al.*, 2010, 2011], and highly porous peaty soils [*Freijer*, 1994] have been measured using the diffusion chamber method. The gas diffusion approach has helped extend the understanding of functional soil structure, and has contributed to the characterization of air-filled pore networks and their dependence on water saturation. However, we are aware of no applications of this

[1]Department of Earth and Environmental Sciences, University of Texas at Arlington, Arlington, Texas, USA.
[2]Graduate School of Science and Engineering, Saitama University, Saitama, Japan.

0043-1397/12/2011WR011098

approach to consolidated porous media. In this study, the diffusion chamber method was adapted to study the diffusivity of nine rock samples and three samples of construction materials (red brick and concretes), using a modified PVC sample holder in the experimental work. In addition, 11 repacked sediments and sands were also examined, using a conventional stainless steel sample holder, to explore the relationship of diffusivity and porosity as given by Archie's law. Correlation of diffusivity to pore size and pore size distribution was also explored to investigate the effect of pore structure on diffusion.

2. Materials and Methods

2.1. Rock, Construction Material, and Sediment Samples

[6] Rock samples studied in this work, including sedimentary (sandstones, chalks, and mudstones) and igneous (tuff and basalt) types, are listed in Table 1, together with the construction materials and repacked sediment samples that were studied. Cylindrical cores (2.5 cm diameter, from 2.0 to 4.2 cm in height) were cored and machined from the rock samples and construction materials. The external cylindrical surface of the core was coated with quick-cure transparent epoxy to prevent lateral diffusion. The rock samples exhibit a range of porosity and permeability, measured by Core Laboratories Inc. (Aurora, Colorado). According to standard procedures of *American Petroleum Institute* [1960], the core sample was placed in a Coberly-Stevens Boyle's law porosimeter and injected with helium at approximately 100 psig. Corresponding pressures and volumes were measured and utilized in the Boyle's law equation to calculate sample grain volume. Pore volume was determined by subtracting the grain volume from the measured bulk volume (determined by Archimedes Principle using mercury immersion), and the total porosity was then calculated from the grain and bulk volumes. For the three construction materials, porosity by the water saturation method was determined by weighing the sample (1) dried at 60°C, (2) then vacuum saturated, and (3) then saturated and submerged to obtain the bulk sample volume (the method of Archimedes) [*Vennard and Street*, 1975]; this approach measures porosity denoting the maximum rock void volume connected to the surface.

[7] Sediment samples (<8 mm fraction) were collected from the lower part of the vadose zone (~3–4 m below ground surface) at the Integrated Field-Scale Research Challenge site at the Hanford 300 Area in Richland, Washington. Samples were air-dried and dry sieved into five size classes of <75 μm, 75–500 μm, 500–2000 μm, <2 mm, and 2–8 mm. These sediment samples, as well as three air-dried silica sands (U.S. Silica, Ottawa, Illinois), were packed in stainless steel sample holders (inner diameter of 5 cm and height of 5 cm) with different bulk densities to obtain different porosities by assuming the particle density of 2.65 g cm^{-3} (Table 1).

2.2. Diffusion Chamber Method for Consolidated Samples

2.2.1. Theoretical Background on Diffusion Coefficient and Diffusivity

[8] For diluted (trace) gas diffusion or diffusion of two gases in a closed system (i.e., where total pressure remains constant), Fick's law, a restrictive case of the Maxwell-Stefan equation, can be applied [*Rolston and Moldrup*, 2002]. Parameter D_p is the gas diffusion coefficient in the porous media [$L^2\ T^{-1}$], which is related to the diffusion coefficient in air D_a by [*Hu and Wang*, 2003]

$$D_P = \tau\sigma\phi_a D_a, \tag{1}$$

where τ denotes tortuosity (<1 herein) and ϕ_a is air-occupied porosity, which is equal to porosity herein since all samples tested were air-dried (modifying ϕ_a value to account for air humidity for rocks with finer pores is discussed in section 3.2.1). Here σ is constrictivity factor, which can be approximated as 1 for pores larger than 1 nm [*Grathwohl*, 1998].

Table 1. Sample Source, Type, and Cylindrical Core Height Used for Gas Diffusion Measurement

Sample	Source[a]	Type	Height (cm)
Gray chalk	Negev Desert, Israel	sedimentary	4.2
White chalk	Negev Desert, Israel	sedimentary	4.2
Zeolitized tuff	Nevada Test Site, Mercury, Nevada	igneous-extrusive	4.0
Mudstone 1	Japan (130 m bgs)	sedimentary	4.0
Mudstone 2	Japan (358 m bgs)	sedimentary	3.9
Berea sandstone	Berea Quarry, Ohio	sedimentary	2.5
Dolomite	Unknown	sedimentary	4.0
Indiana sandstone	Lombard, Illinois	sedimentary	4.0
Basalt	Costa Rica	igneous-extrusive	3.3
Red brick	made from North Carolina red Triassic clay, Durham, North Carolina	construction material	2.8
BART concrete	tunnel wall of Bay Area Rapid Transient, California	construction material	3.0
Asphalt concrete	Laboratory pressed	construction material	4.0
2–8 mm	Hanford Site, Richland, Washington	repacked sediment	5.0
<2 mm	Hanford Site, Richland, Washington	repacked sediment	5.0
500 μm to 2 mm	Hanford Site, Richland, Washington	repacked sediment	5.0
75–500 μm	Hanford Site, Richland, Washington	repacked sediment	5.0
<75 μm	Hanford Site, Richland, Washington	repacked sediment	5.0
53–212 μm	U.S. Silica Company, Ottawa, Illinois	repacked silica sand	5.0
212–300 μm	U.S. Silica Company, Ottawa, Illinois	repacked silica sand	5.0
600–850 μm	U.S. Silica Company, Ottawa, Illinois	repacked silica sand	5.0

[a]Here bgs indicates below ground surface.

[9] The ratio of D_p/D_a is defined as diffusivity, D'. Except for samples with small pores ($<\sim$0.4 nm), where selective gas diffusion will occur because of the activated diffusion and/or molecular sieve-like mechanism [*Burchell et al.*, 1997; *Sircar et al.*, 1996; *Shieh and Chung*, 1999], diffusivity is independent of the gas properties, as discussed by *Boving and Grathwohl* [2001] and *Shimamura* [1992]. Therefore, the diffusivity can be measured by measuring the diffusion coefficient D_p in rocks of a specific gas.

[10] Expressed in Archie's law, D' is found to correlate with porosity [e.g., *Grathwohl*, 1998]:

$$D' = D_p/D_a = \phi_a^m, \tag{2}$$

where m is the cementation factor determined experimentally by fitting the data of diffusivity and porosity. *Buckingham* [1904] gave a universal number of 2 for different repacked and intact variably textured natural soils. However, other values of m have been reported, ranging from as low as 1.33 for soils [*Millington and Quirk*, 1964; *Hamamoto et al.*, 2010], 1.92–2.93 for limestone and sandstone [*Boving and Grathwohl*, 2001], and 2.5–5.4 for clays [*Ullman and Aller*, 1982; *Adler et al.*, 1992; *Horseman et al.*, 1996].

2.2.2. Diffusion Coefficient Measurement for Rocks With Diffusion Chamber Method

[11] The basic setup for rock sample measurement was the same as described by *Rolston and Moldrup* [2002] for soil samples (Figure 1a), except that the stainless steel sample holder was replaced by a PVC core holder (Figure 1b). The diffusion chamber was initially flushed with nitrogen and the oxygen concentration inside the chamber was measured to obtain the intake rate of atmospheric oxygen through the sample. The results were then analyzed on the basis of the following equation [*Rolston and Moldrup*, 2002]:

$$C_r = \frac{C_t - C_s}{C_p - C_s} = \sum_{n=1}^{\infty} \frac{2h\exp(-D_p\alpha_n^2 t/\phi_a)}{L(\alpha_n^2 + h^2) + h}, \tag{3}$$

where C_t and C_0 are oxygen concentrations in the diffusion chamber at times t and 0, respectively. An oxygen sensor (model Figaro KE-12, GS Yuasa, Japan) was used to detect the oxygen concentration, which was recorded with a CR 1000 data logger (Campbell Scientific, Inc., Logan, Utah). C_s is the atmospheric oxygen concentration (20.93% at a normal condition). L is the length of rock sample; $h = \phi_a/\alpha$, in which a is the volume of the chamber per area of rock sample. α_n is the positive root of $(\alpha_n)\tan(\alpha_n L) = h$. The terms for $n \geq 2$ are negligible compared to the first term at some time greater than zero, and equation (3) reduces to

$$C_r = \frac{2h\exp(-D_p\alpha_n^2 t/\phi_a)}{L(\alpha_n^2 + h^2) + h}. \tag{4}$$

Thus, ln C_r becomes linear with t, with the slope of $-D_p\alpha_1^2/\phi_a$ from which D_p can be obtained with known values of α_1 and ϕ_a.

[12] When the diffusion system was originally designed, the slide (Figure 1) was provided to open and close the path between the sample and the diffusion chamber; however, this proved impractical in operation and created major leakage in the system (R. P. Ewing, Iowa State University, personal communication, 2011). Therefore, in our experiments the slide was kept in the open position at all times. Nitrogen was admitted to the chamber at low pressure with both the inlet and outlet ports open; approximately one to two minutes were required for nitrogen to completely fill the chamber, as indicated by a stable oxygen sensor signal of $\sim$0.1 mV. At this point, the inlet port was first switched off, followed by the outlet port, to prevent pressure buildup inside the diffusion chamber. Advection of nitrogen in the rock sample, if any, would be minimal under these procedures considering the short nitrogen filling duration relative to the long diffusion process (usually hours to 1 day).

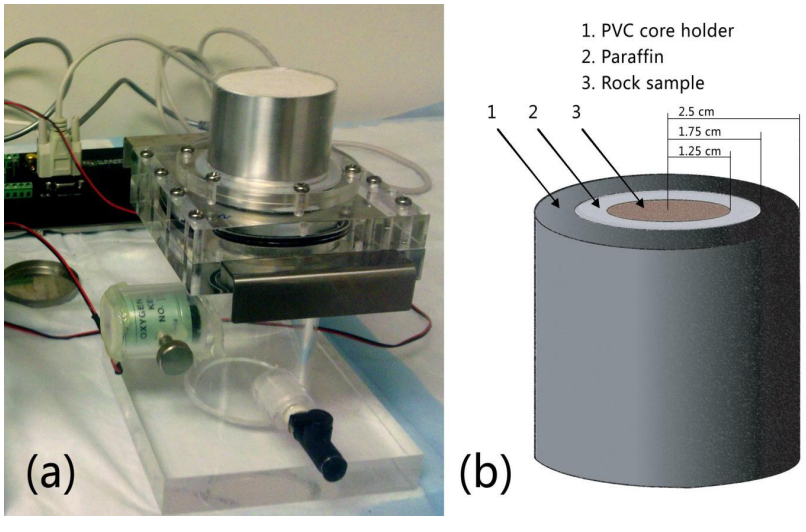

Figure 1. Experimental setup. (a) The whole gas diffusion setup (Plexiglas chamber at the bottom, oxygen sensor to the left of the chamber, metal slide at the front to open and close between chamber and sample; shown with the sand packed in a stainless steel sample holder). (b) PVC core holder assembly for consolidated samples.

[13] The sample holder for consolidated samples was fabricated from PVC, with an inner diameter of 3.5 cm and a height from 2 to 4 cm to fit different samples (Figure 1b). The outer diameter of the PVC sample holder, 5 cm, closely fits the base set of the chamber apparatus. Rock and construction material samples were placed at the center of the PVC holder; after which heated liquid paraffin was carefully poured into the gap between the sample and the holder. Two additional steps were implemented before the paraffin pouring to minimize system leakage: the PVC sample holder was grooved horizontally along its entire inner wall to increase the roughness for better contact between the paraffin and the PVC (to minimize diffusion along the wall); and samples were wrapped tightly with a thin paraffin tape, which would melt in the poured hot paraffin, in order to achieve a tight contact between the sample and the paraffin. After the paraffin had solidified, a firm push by hand was applied to the base of the sample to check the tightness of fit; the sample and PVC holder were reassembled in response to any indication of loose contact. A solid cylindrical core made of PVC, which is considered nonporous, was used to evaluate the system leakage, the result of which then served as the baseline and was subtracted from the sample measurement results to correct for the system leakage effect. All the experiments were conducted under room temperature of 22.5 ± 0.5°C.

2.3. Pore Size Distribution Determination

[14] For tuff and mudstone 1 with very fine pores, the pore size distribution (PSD) was measured through a set of water retention curves, following the water absorption isotherm method [*Kate and Gokhale*, 2006]. PSD for others rock samples were obtained on the basis of the cumulative intrusion volume measured under each pressure step using a mercury intrusion porosimetry (AutoPore IV 9510, Micromeritics, Norcross, Georgia). The pore throat diameter was calculated according to Washburn's equation [*Washburn*, 1951], with the mercury surface tension of 485 dynes/cm and contact angle of 130°. The PSD for mudstone 1 was also measured with the mercury intrusion method to check the consistency of the two methods.

3. Results and Discussion

3.1. System Leakage Test of the Diffusion Chamber

[15] System leakage arises primarily because of the apparatus-sample contacts and inlet and outlet of the gas diffusion chamber. In addition to the steps outlined in section 2, adequate vacuum grease was applied in all contacts and the screws were fastened to seal the sample holder tight to reduce the system leakage to the largest extent. Triplicate experiments using the solid PVC core sample, with the same procedure as the sample, were conducted to examine the system leakage. As shown in Figure 2, the oxygen intake slowly rises from 0.1 mV to approximately 2.0 mV after 2 days; this is minor compared to that of most samples (up to 27.5 mV within a day or so). However, the diffusion signal of asphalt concrete basically overlaps that of the system leakage. Therefore, the system leakage, which is equivalent to a diffusion coefficient of 4.8×10^{-9} m^2 s^{-1} for samples with a diameter of 2.5 cm and height of 4 cm, sets the method detection limit. We suggest 2 times of the

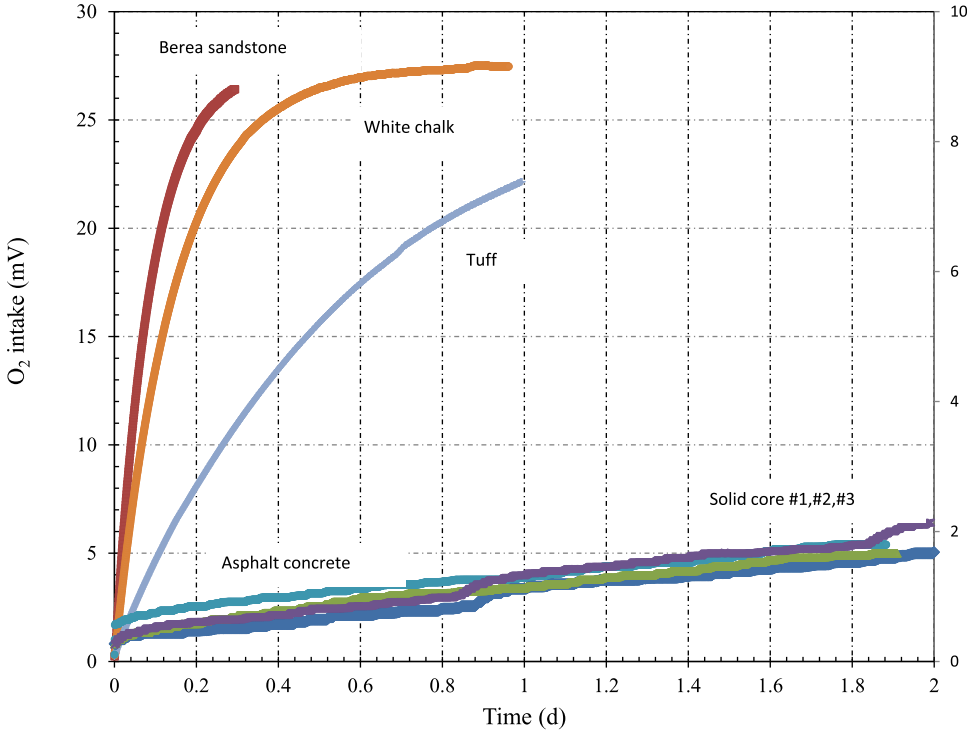

Figure 2. Examples of oxygen intake signal by the KE-12 sensor in diffusion tests: three rock samples refer to left *y* axis; asphalt concrete and three solid PVC cores refer to right *y* axis. Oxygen signal of 27.5 mV corresponds to a saturated atmospheric oxygen concentration (20.95%), while ~0.1 mV corresponds to a nominal oxygen concentration of 0%.

equivalent diffusion coefficient of the system leakage as the detection limit; therefore, a diffusion coefficient as low as 9.6×10^{-9} m^2 s^{-1} can be measured for consolidated samples with a diameter of 2.5 cm and a height of 4 cm. This value corresponds to diffusivity of 4.7×10^{-4} with a D_a value of 2.04×10^{-5} m^2 s^{-1} for oxygen, which will cover most consolidated samples except for tight ones (e.g., granite, shale). With different configurations of diffusion chamber and sample dimension, the detection limit will be different.

3.2. Measured Diffusivity and Its Correlation to Porosity and Pore Size Distribution

[16] The time for ln C_r to achieve linearity with t (as described by equation (4)) was calculated to be 3–5 min for all the experiments using equation (4.3-6) of *Rolston and Moldrup* [2002]. As shown in Figure 3, ln C_r is linear with t which in turn justifies the validity of the experimental approach; values of R^2 for the linear regression are mostly larger than 0.99. The good linearity also indicates the minimal influence of temperature perturbation in the laboratory. The steeper slopes indicate larger diffusion coefficients, D_p. The diffusion coefficients, calculated from the slopes as described in section 2.2.2, are presented in Table 2. The asphalt concrete sample has the minimal D_p ($<9.8 \times 10^{-9}$ m^2 s^{-1}), while red brick has the largest D_p (1.44×10^{-6} m^2 s^{-1}), which is of the same magnitude as the repacked sediments and sands (from 2.21×10^{-6} to 4.69×10^{-6} m^2 s^{-1}). Diffusivity was then calculated with a D_a value of 2.04×10^{-5} m^2 s^{-1} for oxygen.

[17] Figure 4 shows the relation between diffusivity and porosity for our data, as well as literature data obtained using aqueous phase tracer method, as indicated in the legend. An observation of Figure 4 reveals that most of the sediment and sand samples display the same trend as that of loamy sand reported by *Kristensen et al.* [2010]; both basically follow Archie's law with $m = 2$. However, some of the sediments appear to follow more closely the line with $m = 2.25$, which was reported by *Boving and Grathwohl* [2001] for their limestone samples. On the other hand, the rock and construction material samples show more scatter: red brick and Berea sandstone are in line with those sands and sediments, while mudstones and tuff show a much larger m value (around 3.95). The scattering feature is expected since the value of m is different for different type of rocks and pore geometries. Even for the rocks of the same type, there is still a substantial scatter for the m value as shown by the data of *Witthuser et al.* [2003], in which diffusivity for white and gray chalks (from sources similar to those in our work) were measured using liquid tracers. The high m value for mudstones and tuff may be attributed to Knudsen flow, which will take place in pores under 10 – 100 nm, the mean free path length of gas molecules at room temperature and pressure [*Dullien*, 1979]. However, the diffusivities of white and gray chalks measured in our work (data points in red ellipsoid; Figure 4) are in line with Witthuser et al.'s data (diamond data points), which are obtained from aqueous phase tracer method, indicating the insignificant effect of Knudsen flow in white and gray chalks. This also confirms the validity of the gas diffusion approach compared to the traditional aqueous phase tracer approach for consolidated samples.

[18] Figure 5 shows the results of pore size distribution for some rocks and construction materials. Observation of Figure 5 reveals that most of the samples measured herein have a wide range of pore size distribution, except for the gray and white chalks, for which more than 90% of the pore size is in the narrow range from 0.1 μm to 0.67 μm.

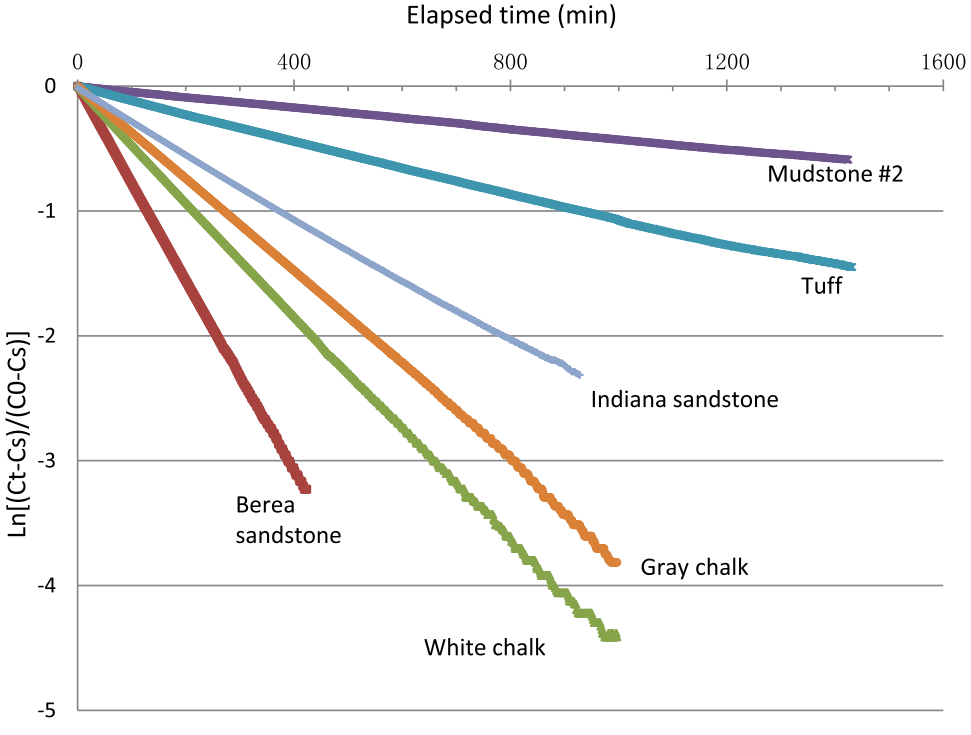

Figure 3. Examples of linear ln C_r versus experimental time for consolidated samples.

Table 2. Measured Porosity, Diffusion Coefficient, and Archie's Law Coefficient *m*

Sample	Porosity (Air Porosity)[a]	D_p[b] (m^2 s^{-1})		*m*
		Average	SD	
Gray chalk	0.396	7.36E−7	1.02E−7	3.59
White chalk	0.456	9.53E−7	3.15E−8	3.90
Zeolitized tuff	0.29 (0.26)	2.58E−7 (2.57E−7)	NA	3.57 (3.28)
Mudstone 1	0.33 (0.30)	9.69E−8 (9.68E−8)	NA	4.89 (4.44)
Mudstone 2	0.38 (0.345)	3.69E−7 (3.63E−7)	3.81E−8	4.18 (3.78)
Berea sandstone	0.228	1.00E−6	NA	2.04
Dolomite	0.093	3.00E−7	4.39E−8	1.78
Indiana sandstone	0.174	5.31E−7	5.86E−9	2.09
Basalt	0.0419	1.40E−8	NA	2.30
Red brick	0.203	1.44E−6	3.80E−8	1.66
BART concrete	0.158	1.10E−7	NA	2.83
Asphalt concrete	0.0218	<9.8E−9	NA	NA
2–8 mm	0.431	3.93E−6	3.96E−8	1.96
2–8 mm	0.424	3.53E−6	1.11E−7	2.04
<2 mm	0.431	3.92E−6	2.70E−7	1.96
500 μm to 2 mm	0.431	3.83E−6	5.85E−8	1.99
500 μm to 2 mm	0.471	4.45E−6	2.35E−7	2.02
75–500 μm	0.431	3.10E−6	4.08E−8	2.24
75–500 μm	0.522	4.69E−6	1.94E−7	2.26
<75 μm	0.525	4.09E−6	9.84E−8	2.49
53–212 μm	0.42	2.21E−6	1.59E−7	2.56
212–300 μm	0.44	3.93E−6	1.02E−7	2.01
600–850 μm	0.378	4.09E−6	8.54E−8	1.65

[a]Air porosity is equal to measured porosity, except for tuff and mudstones to account for the initial saturation effect. For unconsolidated samples, porosities were obtained from the sample weight packed in cylindrical core holder (5 cm inner diameter and 5 cm long).
[b]Read 1.19E−7 as 1.19×10^{-7}; NA, not available.

Indiana sandstone has the largest pores (with d_{50}, the volumetric mean pore diameter, of 21.8 μm), while the mudstones and tuff have the smallest pores (d_{50} of 0.014 μm). The PSD for mudstone 1 from the mercury intrusion generated slightly larger pore size distribution than the water absorption method; however, the two methods produced a similar d_{50} value of approximately 0.04 μm. The samples were air-dried and therefore were not completely devoid of moisture. During the course of the experiments, the laboratory humidity was around ∼45%, which according to

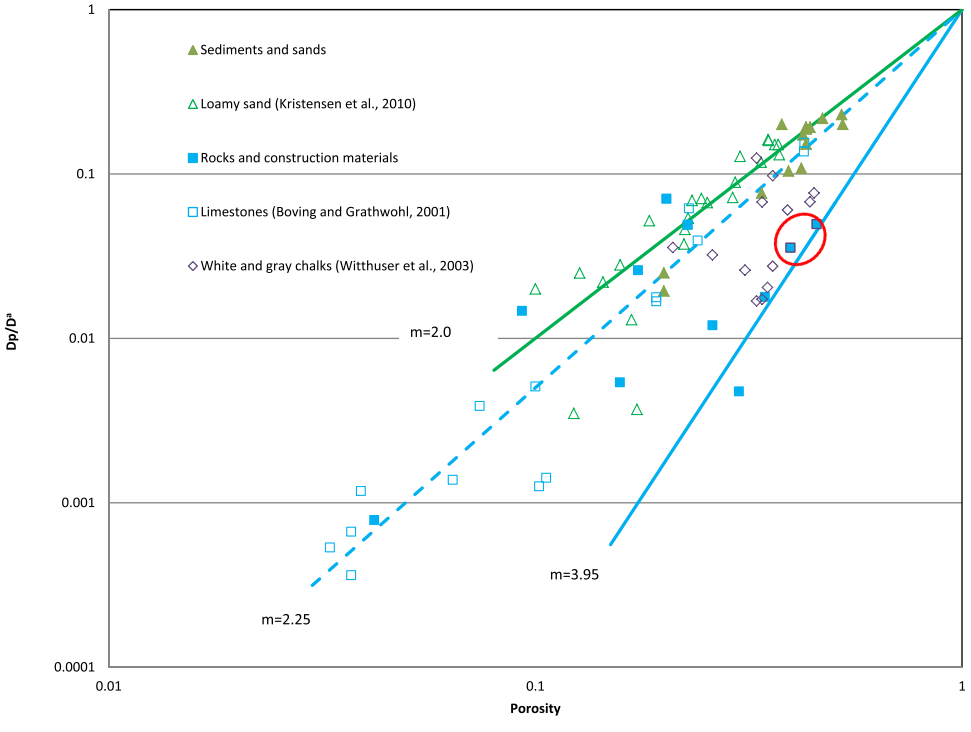

Figure 4. Relationship of diffusivity and porosity. Lines are estimation by Archie's law with different *m* values. Solid symbols are measured values in this work, and open symbols are obtained from studies listed in the legend. Data in the red ellipsoid are gray and white chalk diffusivities from our study.

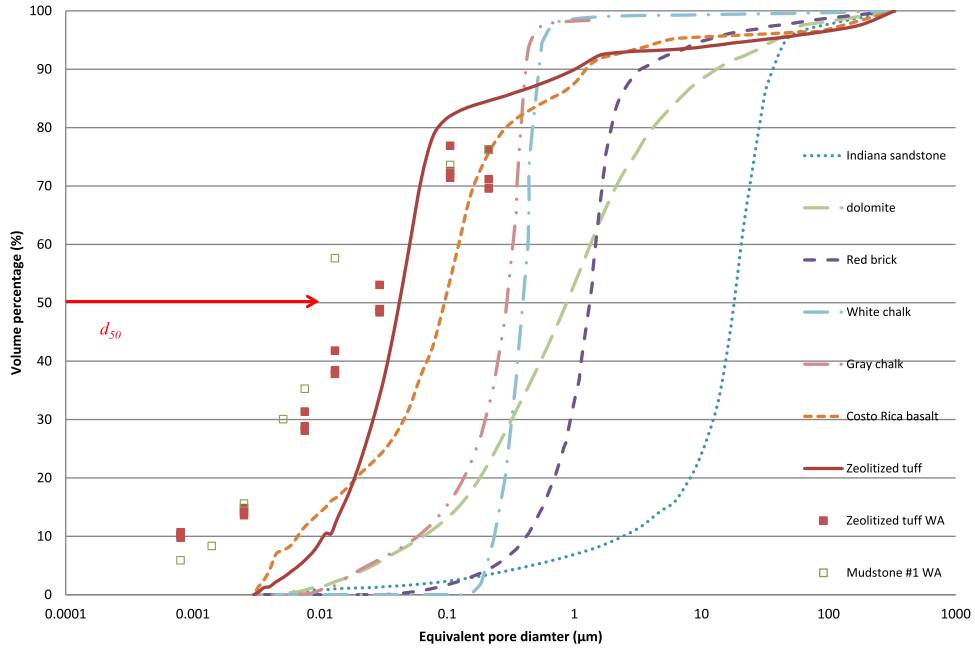

Figure 5. Pore size distribution for selected rocks and construction materials. WA, water absorption method.

Kelvin's equation, with corresponding pore diameters of <1.2 nm were filled with water. For mudstones and tuff, 1.2 nm accounts for approximately 10% of the porosity. Therefore, the air porosity values for mudstones and tuff were modified, which accordingly affects the diffusion coefficients (values in parenthesis in Table 2).

[19] The m value for each sample was calculated using Archie's law (equation (2)); the results are listed in Table 2. The range of m is from 1.66 to 4.44 for rock and construction materials; for sediments and sands, the range is from 1.65 to 2.56. A plot of m versus d_{50} for the rocks and construction materials is shown in Figure 6. For most of the

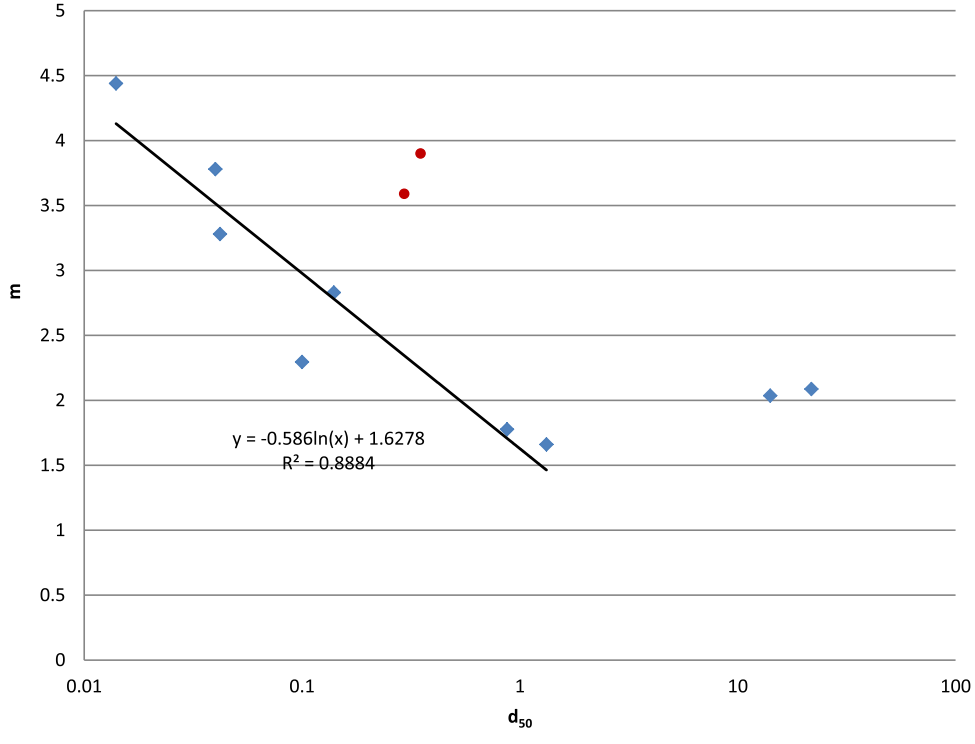

Figure 6. Semilog relationship between m value and d_{50}. A linear relationship can be found for most samples with $d_{50} < 1.3$ μm expect gray and white chalks (circles), which have relatively narrower pore size distribution.

samples, the m value decreases with an increasing ln d_{50} in an approximately linear manner for values of d_{50} less than 1.3 μm, as shown by the following relationship:

$$m = -0.59 \ln d_{50} + 1.63. \quad (5)$$

The two outliers in Figure 6 are gray and white chalks, which were shown to have narrower pore size distributions than other rocks. For rocks with d_{50} values greater than 1.3 μm, the value of m becomes close to 2.0. This is consistent with the observations that many coarse rocks have m values around 2.0, similar to those of coarse sediments and sands. On the contrary, rocks with smaller pores tend to have greater m value. This indicates that the diffusivity is affected not only by porosity, but also by pore size and pore size distribution; larger pores usually correlate to smaller tortuosity and better connectivity of the pore structure and therefore lead to a larger diffusivity. This is also true for the Hanford sediments; for example, the <75 μm Hanford sediment has a larger m value (2.49) than coarser sediments (from 1.96 to 2.26); and the fine-grained 212–300 μm (50–70 mesh) silica sand has a larger m value (2.56) than the coarse-grained 600–850 μm (20–30 mesh) silica sand (1.65 and 2.01).

4. Conclusions

[20] In this work, the diffusion chamber method with oxygen as the tracer gas was successfully used to measure diffusion coefficients of 12 air-dried rocks and construction materials. Careful assembly of the samples and the sample holder, with the help of paraffin and vacuum grease, were utilized to reduce the system leakage to the maximum extent possible. The resultant diffusion coefficients range from $<9.8 \times 10^{-9}$ m^2 s^{-1} (the detection limit with the experimental system and approach) to 1.44×10^{-6} m^2 s^{-1}. Diffusion coefficients were also measured for 11 sediment and sand samples with different particle sizes and compaction, with the results varying from 2.21×10^{-6} to 4.69×10^{-6} m^2 s^{-1}. The measurement usually took less than a day for the oxygen to reach equilibrium with atmosphere, much faster than the aqueous phase tracer method.

[21] Diffusivity for both rock and construction materials is related to porosity, in the form of Archie's law; however, the m value varies to some extent. Rock samples with finer pores have larger m values (up to 4.9 for mudstone 1); conversely, rock samples (Berea sandstone and red brick) with coarser pores have smaller m values in the proximity of 2.0. The m values for repacked sands and sediments are smaller, ranging from 1.65 to 2.56. As in the consolidated samples, the m values are larger for unconsolidated samples with coarser pores than for those with finer pores. For most of the rock samples for which the volumetric mean diameter, $d_{50,}$ was less than 1.3 μm, a linear regression equation (equation (5)) was found to describe the m value in terms of ln d_{50}; however, this equation underestimates the m value for gray and white chalks which have a relatively narrower pore size distribution. This indicates that both the mean pore size (d_{50}) and the pore size distribution have a significant influence on the diffusivity.

[22] **Acknowledgments.** This research was supported by the Subsurface Biogeochemical Research program DE-SC0005394, Office of Biological and Environmental Research, U.S. Department of Energy, for project ER65073. This work was also partially funded by the Japan Society for the Promotion of Science bilateral research project.

References

Adler, P. M., C. G. Jacquin, and J. F. Thovert (1992), The formation factor of reconstructed porous media, *Water Resour. Res.*, *28*(6), 1571–1576.

American Petroleum Institute (1960), Recommended practice for core analysis procedure, *Recomm. Prac. 40*, Dallas, Tex.

Becker, M., and A. Shapiro (2000), Tracer transport in fractured crystalline rock: Evidence of non-diffusive breakthrough tailing, *Water Resour. Res.*, *36*(7), 1677–1686.

Boving, T. B., and P. Grathwohl (2001), Tracer diffusion coefficients in sedimentary rocks: Correlation to porosity and hydraulic conductivity, *J. Contam. Hydrol.*, *53*, 85–100.

Buckingham, E. (1904), *Contributions to Our Knowledge of the Aeration of Soils, Bur. Soil Bull. 25*, U.S. Gov. Print Off., Washington, D. C., 52 pp.

Burchell, T. D., R. R. Judkins, M. R. Rogers, and A. M. Williams (1997), A novel process and material for the separation of carbon dioxide and hydrogen sulfide gas mixtures, *Carbon*, *35*, 1279–1294.

Conca, J., R. Jacob, and M. Johnson (2004), Reducing the threat of a serious ^{137}Cs dirty bomb, paper presented at Working Together: Research & Development (R&D) Partnerships in Homeland Security, Dep. of Homeland Security, Boston, Mass., 27–28 April. [Available at http://www.cemrc.org/dirtybomb/dirtybomb_conca.htm.]

Cui, X., R. Bustin, and G. Dipple (2004), Selective transport of CO_2, CH_4, and N_2 in coals: Insights from modeling of experimental gas adsorption data, *Fuel*, *83*, 293–303.

Cui, X., A. Bustin, and R. Bustin (2009), Measurements of gas permeability and diffusivity of tight reservoir rocks: Different approaches and their applications, *Geofluids*, *9*, 208–223.

Dullien, F. A. L. (1979), *Porous Media Fluid Transport and Pore Structure*, Academic, New York.

Freijer, J. I. (1994), Calibration of jointed tube model for gas diffusion coefficient in soils, *Soil Sci. Soc. Am. J.*, *58*, 1067–1076.

Gillham, R. W., M. L. J. Robin, D. J. Dytynyshyn, and H. M. Johnson (1984), Diffusion of nonreactive and reactive solutes through fine-grained barrier materials, *Can. Geotech. J.*, *21*, 541–550.

Grathwohl, P. (1998), *Diffusion in Natural Porous Media: Contaminant Transport, Sorption/Desorption and Dissolution Kinetics*, 224 pp., Kluwer Acad., Boston, Mass.

Hamamoto, S., P. Moldrup, K. Kawamoto, and T. Komatsu (2010), Excluded-volume expansion of Archie's law for gas and solute diffusivities and electrical and thermal conductivities in variably saturated porous media, *Water Resour. Res.*, *46*, W06514, doi:10.1029/2009WR008424.

Hamamoto, S., P. Moldrup, K. Kawamoto, L. W. de Jonge, P. Schjonning, and T. Komatsu (2011), Two-region extended Archie's law model for soil air permeability and gas diffusivity, *Soil Sci. Soc. Am. J.*, *75*, 795–806.

Hatiboglu, C. U., and T. Babadagli (2010), Experimental and visual analysis of diffusive mass transfer between matrix and fracture under static conditions, *J. Petrol. Sci. Eng.*, *74*, 31–40.

Horseman, S. T., J. J. W. Higgo, J. Alexander, and J. F. Harrington (1996), Water, gas and solute movement through argillaceous media, *NEA/OECD Rep. CC-96/1*, Nucl. Energy Agency, Washington, D. C.

Hou, K., M. Fowles, and R. Hughes (1999), Effective diffusivity measurements on porous catalyst pellets at elevated temperature and pressure, *Chem. Eng. Res. Design*, *77*, 55–61.

Hu, Q. H., and J. S. Y. Wang (2003), Aqueous-phase diffusion in unsaturated geologic media: A review, *Crit. Rev. Environ. Sci. Technol.*, *33*(3), 275–297.

Kate, J. M., and C. S. Gokhale (2006), A simple method to estimate complete pore size distribution of rocks, *Eng. Geol.*, *84*(1–2), 48–69.

Kristensen, A. H., A. Thorbjørn, M. P. Jensen, M. Pedersen, and P. Moldrup (2010), Gas-phase diffusivity and tortuosity of structured soils, *J. Contam. Hydrol.*, *115*, 26–33.

Mair, R. W., M. D. Hurlimann, P. N. Sen, L. M. Schwartz, S. Patz, and R. L. Walsworth (2001), Tortuosity measurement and the effects of finite pulse widths on xenon gas diffusion NMR studies of porous media, *Magn. Reson. Imaging*, *19*, 345–351.

Millington, R. J., and J. P. Quirk (1964), Formation factor and permeability equations, *Nature*, *202*, 143–145.

Moldrup, P., T. Olesen, H. Blendstrup, T. Komatsu, L. W. de Jonge, and D. E. Rolston (2007), Predictive-descriptive models for gas and solute diffusion coefficients in variably saturated porous media coupled to pore-size distribution: IV. Solute diffusivity and the liquid phase impedance factor, *Soil Sci.*, *172*, 741–750.

Mouchot, N., and A. Zoulatian (2002), Longitudinal permeability and diffusivity of steam in beech determined with a Wicke-Kallenbach cell, *Holzforschung*, *56*, 318–326.

Nestle, N., P. Galvosas, P., O. Geier, M. Dakkouri, C. Zimmermann, and J. Kärger (2001a), NMR studies of water diffusion and relaxation in hydrating slag-based construction materials, *Magn. Reson. Imaging*, *19*(3–4), 547–548.

Nestle, N., C. Zimmermann, M. Dakkouri, and R. Niessner (2001b), Action and distribution of organic solvent contaminations in hydrating cement: Time-resolved insights into solidification of organic waste, *Environ. Sci. Technol.*, *35*, 4953–4956.

Newling, B. (2008), Gas flow measurements by NMR, *Prog. Nucl. Magn. Reson. Spectrosc.*, *52*, 31–48.

Polak, A., R. Nativ, and R. Wallach (2002), Matrix diffusion in northern Negev fractured chalk and its correlation to porosity, *J. Hydrol.*, *268*, 203–213.

Rolston, D. E., and P. Moldrup (2002), Gas diffusivity, in *Methods of Soil Analysis: Part 4, Physical Methods*, edited by J. H. Dane and G. C. Topp, pp. 1113–1139, Soil Sci. Soc. of Am., Madison, Wis.

Salejova, G., Z. Grofa, O. Solcovab, P. Schneiderb, and J. Koseka (2011), Strategy for predicting effective transport properties of complex porous structures, *Comput. Chem. Eng.*, *35*, 200–211.

Schlünder, E.-U., J. Yang, and A. Seidel-Morgenstern (2006), Competitive diffusion and adsorption in Vycor glass membranes—A lumped parameter approach, *Catal. Today*, *118*, 113–120.

Shieh, J.-J., and T. S. Chung (1999), Gas permeability, diffusivity, and solubility of poly (4-vinylpridine) film, *J. Polym. Sci., Part B*, *37*, 2851–2861.

Shimamura, K. (1992), Gas diffusion through compacted sands, *Soil Sci.*, *153*, 274–279.

Sircar, S., T. C. Golden, and M. B. Rao (1996), Activated carbon for gas separation and storage, *Carbon*, *34*, 1–12.

Soukup, K., P. Schneidera, and O. Šolcováa (2008), Wicke-Kallenbach and Graham's diffusion cells: Limits of application for low surface area porous solids, *Chem. Eng. Sci.*, *63*(18), 4490–4493.

Ullman, W. J., and R. C. Aller (1982), Diffusion coefficients in nearshore marine sediments, *Limnol. Oceanogr.*, *27*, 552–556.

Vennard, J. K., and R. L. Street (1975), *Elementary Fluid Mechanics*, John Wiley, New York.

Wang, R. P., R. W. Mair, M. S. Rosen, D. G. Cory, and R. L. Walsworth (2004), Simultaneous measurement of rock permeability and effective porosity using laser-polarized noble gas NMR, *Phys. Rev. E*, *70*, 026312.

Wang, R. P., T. Pavlin, M. S. Rosen, R. W. Mair, D. G. Cory, and R. L. Walsworth (2005), Xenon NMR measurements of permeability and tortuosity in reservoir rocks, *Magn. Reson. Imaging*, *23*, 329–331.

Washburn, E. W. (1951), Note on a method of determining the distribution of pore sizes in a porous materials, *Proc. Natl. Acad. Sci. U. S. A.*, *7*, 115–116.

Witthuser, K., B. Reichert, and H. Hotzl (2003), Contaminant transport in fractured chalk: Laboratory and field experiments, *Ground Water*, *41*, 806–815.

Zhang, F., R. E. Hayes, and S. T. Kolaczkowski (2004), A new technique to measure the effective diffusivity in a catalytic monolith wash coat, *Chem. Eng. Res. Des.*, *82*, 481–489.

S. Hamamoto, Graduate School of Science and Engineering, Saitama University, Sakura-ku, Saitama 338-8570, Japan.

Q. Hu and S. Peng, Department of Earth and Environmental Sciences, University of Texas at Arlington, Arlington, TX 76019, USA. (maxhu@uta.edu)